Polymer 51 (2010) 6058–6070

Contents lists available at ScienceDirect

Polymer

journal homepage: www.elsevier.com/locate/polymer

Molecular simulations of crosslinking process of thermosetting polymers

Chunyu Li*, Alejandro Strachan

School of Materials Science and Engineering and Birck Nanotechnology Center, Purdue University, West Lafayette, IN 47906, USA

ARTICLE INFO

Article history:
Received 23 July 2010
Received in revised form
13 October 2010
Accepted 15 October 2010
Available online 23 October 2010

Keywords:
Molecular dynamics simulations
Thermoset polymer
Polymerization

ABSTRACT

We use molecular dynamics (MD) with a procedure to describe chemical reactions to predict the atomic structure and properties of the thermosetting polymer epoxy EPON-862 and curing agent DETDA. The DREIDING force field is employed with environment-dependent atomic charges obtained self consistently during the dynamics. We propose a computationally efficient method to describe charge evolution based on the observation that atomic charges evolve significantly only during chemical reactions and in a repeatable manner. Two chemistry models with different relative rates for primary and secondary amine reactions are used to mimic the curing process in two extreme cases of processing conditions. The simulations show that differences in chemical reaction rates affect properties for intermediate conversion degrees (~40–70%) but not for the higher conversion rates of interest in most applications. We also find that performing the polymerization at high temperatures leads to networks with lower internal strain energy due to increased molecular mobility. The predicted density, coefficient of thermal expansion, glass transition temperature and elastic constants of the resulting polymers are in excellent agreement with experiments.

1. Introduction

Fiber-reinforced polymer composite materials have become increasingly important in aircraft applications because of their advantages in weight reduction and energy saving. For example, the Boeing Company has raised the use of composite materials in new aircrafts up to 50% of structural weight [1]. Thermosetting polymers are the matrices of choice for such composites due to their high stiffness, strength, creep resistance and thermal resistance when compared with thermoplastic polymers [2]. These desirable properties stem from the three-dimensional (3D) crosslinked structures of these polymers. Many thermosetting polymers are formed by mixing a resin (epoxy, vinyl ester, or polyester) and a curing agent. An irreversible chemical reaction cures the two components into a solid polymer with a 3D network of covalent bonds.

The mechanical and physical properties of thermosetting polymers depend on their chemistry, composition, and curing conditions. Taking into account the various resin and curing agent combinations as well as additives to control processing characteristics (e.g. viscosity) and resulting properties, the number of possible formulations is enormous. The optimization of thermoset formulations remains, to a large degree, empirical and based on trial and error leading to lengthy and costly cycles. In this context, physics-based computational tools capable of predicting the properties of new formulations would be highly desirable. Advances in atomistic simulation techniques and the continuing increase in computer power open the possibility of a molecular-level description of these materials. Furthermore, being based on first principles these techniques have the potential to predict the performance of new formulations and to provide guidance to design and optimization efforts. In this paper we develop a procedure based on molecular dynamics (MD) simulations to predict the molecular structure and material properties of thermosetting polymers from first principles. The procedure is applied to the epoxy resin EPON-862 with curing agent DETDA. This choice enables the comparison of our results with available experimental data and prior simulation results. We characterize the role of the polymerization procedure on the internal strain of the generated network and the role of the relative reaction rates for the polymerization chemistry on resulting properties. The predictions (with no adjustable parameters) of glass transition temperature, density, thermal expansion coefficient and elastic constants are in good agreement with available experimental values. It should be pointed out that the polymerization procedure characterized in this paper is generally applicable and can be used to predict other thermosetting polymer systems without modifications.

Initial efforts to study the formation of crosslinked networks with atomic resolution by computer simulations can be traced back to 1980s. A rather thorough review of such works is provided by

* Corresponding author.
E-mail address: licyemail@yahoo.com (C. Li).

0032-3861/$ – see front matter © 2010 Elsevier Ltd. All rights reserved.
doi:10.1016/j.polymer.2010.10.033

Doherty et al. [3]. In these initial studies, all the crosslinking reactions were assumed to occur simultaneously without time for the system to relax as the network is formed; thus, large internal network strains are expected in the resulting configurations. Since Doherty et al. [3] performed simulations allowing a progressive crosslinking and polymerization reaction using MD, several researchers reported studies of crosslinked polymer networks built using molecular dynamics simulations. For example, Yarovsky and Evans [4] developed a methodology for constructing molecular models of crosslinked polymer networks and applied it to low molecular weight water soluble epoxy resins cured with different crosslinking agents. The polymer consistent force field (PCFF) was used and the volume shrinkage during conversion was predicted. Heine et al. [5] simulated the structure and elastic moduli of end-crosslinked PDMS networks. The networks were formed dynamically using MD. The newly formed topology was relaxed using a modified potential, harmonic at bonding distances, below a predetermined cutoff, and linear at larger distances to avoid instabilities when a new bond is formed. Gou et al. [6] built crosslinked polymer matrix with epoxy resins (EPON-862) and curing agents (DETDA) to study interfacial load transfer in carbon nanotubes/polymer composites. Wu and Xu [7] performed crosslinking simulations for epoxy resin system based on DGEBA (diglycidyl ether bisphenol A) and IPD (isophorone diamine). They used the DREIDING force field with charge equilibration to build the structure but COMPASS force field for property prediction. They found that COMPASS provides a more accurate description of elastic properties; however, their DREIDING prediction of Young's modulus (about 50 GPa) is not consistent with our experience as will be described below. Fan and Yuen [8] conducted MD simulations to predict the glass transition temperature (T_g), linear thermal expansion coefficients (CTE) and Young's modulus of fully cured epoxy network composed of EPON-862 epoxy resin and TETA (triethylenetetramine) curing agent. Their simulations used the Material Studio (Accelrys Inc.) with the PCFF force field and their predictions of T_g, CTE and Young's modulus were shown to be within 10% of the experiments. Lin and Khare [9] presented a single-step polymerization method for the creation of atomistic model structures of crosslinked polymers. A simulated annealing algorithm was used to identify pairs of reacting atoms within a cutoff distance and all crosslinking bonds were created in a single step. Recently, Varshney et al. [10] reported a study of molecular modeling of thermosetting polymers with special emphasis on crosslinking procedure. They describe different approaches to build highly crosslinked polymer networks and proposed a multistep relaxation procedure for relaxing newly formed topology in the crosslinking process. Using the consistent valence force field (CVFF), they predicted density, glass transition temperature, and thermal expansion coefficient of an epoxy-based thermoset (EPON-862/DETDA); the predicted T_g is lower than the experimental value. Komarov et al. [11] reported a new computational method where the polymer network is polymerized at a coarse-grained level and then mapped into a fully atomistic model. Molecular dynamics are then carried out with the OPLS force field. The predicted T_g is about 20 K lower than experimental results; this underestimation would increase once the extremely high cooling rates of MD taken into account.

An aspect that has not been fully explored in these crosslinking simulations is the evolution of partial atomic charges during curing. Electrostatic interactions play an important role in the overall binding of these systems and an accurate calculation of charge distribution is essential for the prediction of their structure and properties. In most classical molecular dynamics simulations, static atomic charges are used. However, during polymerization/crosslinking simulations the charge distribution is expected to change

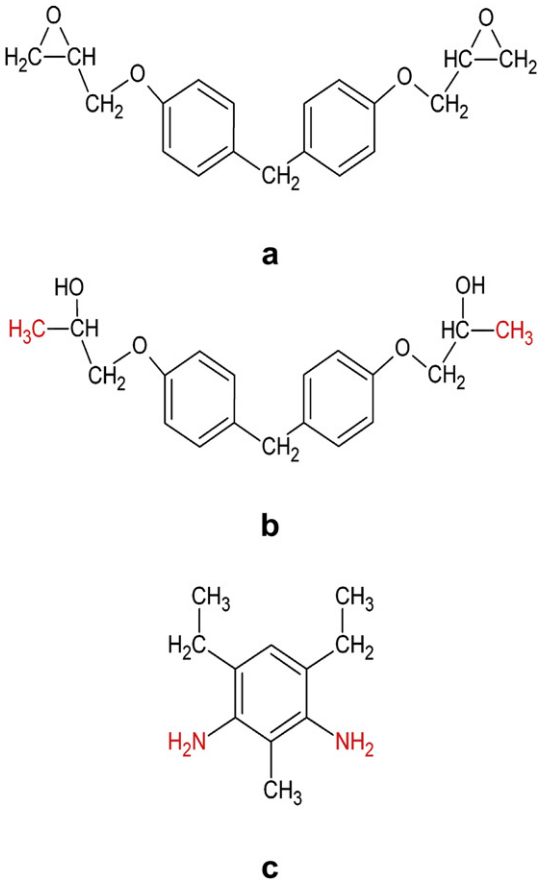

Fig. 1. Molecular structures of (a) EPON-862, (b) activated EPON-862 and (c) DETDA.

when chemical reactions occur [10]. Thus, an accurate simulation of the crosslinking process should include a procedure for updating charges to take into account changes in chemistry and topology. Geometry dependent, self-consistent charges can be obtained by minimizing an expression for the total electrostatic energy using methods like Charge equilibration (QEq) [12] or electronegativity equalization method (EEM) [13–15]. These methods are accurate and transferable and have been applied to polymerization [7] but they remain computationally intensive especially for large-scale simulations. In this paper, we characterized the charge evolution during polymerization of the EPON-862/DETDA system using explicit EEM. We find that charges evolve significantly only during chemical reactions and this evolution is predictable from the chemistry of the reaction and insensitive to the actual atomic configuration of the process. Based on these observations, we propose a computationally efficient charge updating approach, denoted electronegative equalization-based charge assignment (ECA), which enables large-scale polymerization and crosslinking simulations.

2. Computational approach and simulation details

Our overall procedure to predict the atomic structure and thermo-mechanical properties of thermoset polymers consists of three main stages: i) polymerization, where the initial liquid mixture forms a 3D network; ii) annealing, where the polymerized system is cooled down to room temperature and from which we obtain glass transition temperature and thermal expansion coefficients; and iii) mechanical testing, where we use non-equilibrium MD to subject the annealed samples to deformation and from which we obtain elastic constants. The following subsections

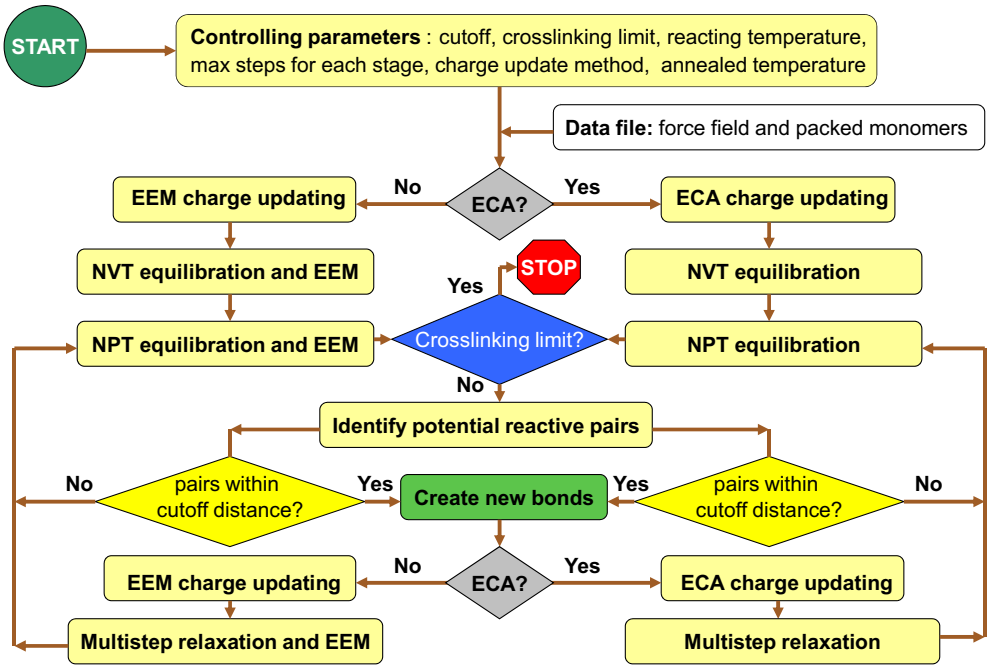

Fig. 2. Flowchart of the simulation procedure for crosslinking process.

describe the system of interest and simulation details of the various stages of our approach and Section 3 describes the polymerization procedure.

2.1. System of interest

This paper focuses on the conversion of stoichiometrically perfect mixtures of EPON-862 (diglycidyl ether of bisphenol F) and curing agent EPI-Cure-W (diethylenetoluenediamine, DETDA). The molecular structures of the two monomers are shown in Fig. 1. To simulate the polymerization and crosslinking process, the potential reactive sites in the epoxy resin are activated by hydrating the epoxy oxygen atoms at the ends of the molecule, see Fig. 1(b). Each of the amine groups in DETDA can react with two epoxy molecules: the initial reaction converts a primary amine to a secondary one and the subsequent reaction leads to a tertiary amine. The activation energy for the primary reaction is typically lower than the secondary one, a difference of 3.7 kcal/mol was obtained from FTIR measurements in a similar system [16,17]. Consequently the rate of the primary reaction can be significantly higher than that of the secondary, especially at low reaction temperatures. In section 3.3 below, we discuss how the relative rates of chemical reaction affect the thermo-mechanical response of the polymers. All our simulations involve systems with perfect stoichiometries, i.e. there are twice as many EPON-862 molecules as DETDA ones. We report results of simulation cells of various size with the following numbers of epoxy and curing molecules (16, 8), (64, 32), (128, 64) and (256, 128). In the expression (n, m), that will be used throughout the paper to identify the various systems, n represents the number of epoxy monomers and m the number of curing agent monomers.

2.2. Atomic interactions

Atomic interactions are described using the DREIDING force field [18]. DREIDING describes the total potential energy of an atomistic systems in terms of: i) bonding interactions including bond stretch, angle bending, torsions involving dihedral angles and improper torsions and ii) non-bond interactions including electrostatics originating from partial atomic charges and van der Waals interactions to describe short range Pauli repulsion and dispersion. DREIDING does not specify partial atomic charges and we use the EEM method to obtain environment-dependent atomic charges for our systems; such a combination of DREIDING with charge equilibration has been successfully used in the past for soft materials, see for example Ref. [19]. The sensitivity of the DREIDING predictions of the liquid density (before polymerization) with respect to the choice of atomic charge is included as Supporting Information; these results show that the choice of partial charges is very important in simulations of these epoxy systems. DREIDING van der Waals interactions have been parameterized with either Lennard–Jones (LJ) or Buckingham (exponential repulsion and inverse sixth power attraction, X6) functions. The polymerization procedure is performed with LJ functional with inner and outer cutoffs of 8 Å and 12 Å respectively and a switching function that take the potential and force to zero between the inner and outer cutoffs. The same approach is used for the calculation of electrostatic interactions. For the annealing and mechanical testing simulations from which thermo-mechanical properties are computed, we use X6 van der Waals potentials (the preferred form for DREIDING) with a cutoff of 12 Å, together with an accurate description of the long-range electrostatics interactions using the pppm method as implemented in LAMMPS [20]. Thus, we favor computationally less intensive choices for the polymerization procedure where the key goal is to obtain a well-relaxed topology and molecular conformations and perform more accurate simulations to predict thermo-mechanical properties.

The DREIDING force field uses atom types to distinguish identical atoms in different chemical environments and we use additional atom types to identify reactive atoms. New types indicate reactive carbon atoms as well as reactive nitrogen atoms in primary or secondary amines.

2.3. Model setup and simulation details

The initial model system is built packing both activated epoxy and agent monomers into a simulation cell followed by a structural relaxation using the commercial software MAPS [21]. All subsequent MD simulations are performed by using LAMMPS [22] a massively parallel simulator from Sandia National Laboratories. In all simulations, 3D periodic boundary conditions are imposed to remove possible surface effects. A Nose–Hoover thermostat [23] with 100 fs coupling constant and Nose–Hoover barostat [24] with 350 fs coupling constant are used for temperature and pressure control respectively.

3. Polymerization and crosslinking procedure

The polymerization procedure can be divided into three main stages: pre-curing equilibration, curing, annealing of the network polymer. Fig. 2 shows the flowchart of the simulation procedure both for EEM and ECA charge updating methods.

3.1. Overall polymerization and crosslinking procedure

3.1.1. Step 1: pre-chemistry equilibration

After packing the desired number of resin and curing agent monomers into a 3D periodic simulation cell at low density (0.5 g/cm^3) the system is equilibrated using isothermal and isochoric (NVT ensemble) MD simulations for 50 ps followed by an isothermal, isobaric (NPT) simulation for 400 ps at atmospheric pressure that takes the liquid to its equilibrium density.

3.1.2. Step 2: polymerization and crosslinking procedure

After the model system is fully equilibrated in step 1, the polymerization and crosslinking is simulated by periodically performing chemical reactions between reactive atoms during an MD simulation. Chemical reactions are performed in a stepwise manner using a criterion based on atomic distances and, as will be described in detail in Section 3.3 below, the type of chemical reaction (primary or secondary amine reactions). The distance between all pairs of reactive C–N atoms are computed and new bonds are created between all those that fall within a pre-assigned cutoff distance; based on prior work [10] we take this distance to be 5.64 Å, four times the equilibrium C–N bond length. After the new bonds are identified all new additional covalent terms (angles, torsions, and improper torsions) are created and hydrogen atoms from the reactive C and N atoms are removed. As will be described below new bonds are turned on slowly using a multistep relaxation procedure to avoid large atomic forces. Once this is accomplished, or if no reactive pairs are found within the cutoff distance, a 50 ps NPT simulation is performed to let the system relax and equilibrate to it new topology before reactive pairs are checked again for possible new reactions. After each 50 ps equilibration run the termination conditions are evaluated: the processes ends if a predetermined conversion limit or maximum simulation time is surpassed. If the end conditions are not met, another round of chemical reactions begins, see Fig. 2. In practice, the conversion limit is set to 100% and the simulations end based on time.

3.1.3. Step 3: thermalization and annealing

As will be described below crosslinked system is usually built at temperatures larger than the glass transition one. An annealing process is used to cool down the system to room temperature or other desired temperature. This annealing process is also used to predict glass transition temperature and the coefficient of thermal expansion.

Table 1
Parameters used in multigroup multistep relaxations ($r_c^i = r_{vdw} + (2i-1)(r_{cutoff} - r_{vdw})/6$).[a]

Groups	Steps	Effective force constants	Effective bond lengths
Group i (i = 1,2,3)	1	$k_0/5$	r_c^i
	2	$2k_0/5$	$r_0 + 3(r_c^i - r_0)/4$
	3	$3k_0/5$	$r_0 + (r_c^i - r_0)/2$
	4	$4k_0/5$	$r_0 + (r_c^i - r_0)/4$
	5	k_0	r_0

[a] In the equation, r_c^i stands for cutoff distance for group i. r_{vdw} is taken as 3.0 Å and r_{cutoff} is 5.64 Å.

3.2. Multi-step bond creation approach

When a new bond is formed between a pair of reactive atoms their separation distance is significantly larger than the equilibrium bond length. Thus, in order to avoid large interatomic forces between the newly connected atoms we use a multistep relaxation procedure similar to the one reported by Varshney et al. [10] where bonds are created in five incremental steps. Furthermore, we divide the reactive pairs that fall between the cutoff distance, r_{cutoff}, and the distance r_{vdw}, at which the interatomic van der Waals potential is zero, into three groups:

$$\begin{cases} \text{Region 1:} & 0 < r \le r_{vdw} + \left(r_{cutoff} - r_{vdw}\right)/3 \\ \text{Region 2:} & r_{vdw} + \left(r_{cutoff} - r_{vdw}\right)/3 < r \le r_{vdw} + 2\left(r_{cutoff} - r_{vdw}\right)/3 \\ \text{Region 3:} & r_{vdw} + 2\left(r_{cutoff} - r_{vdw}\right)/3 < r \le r_{cutoff} \end{cases}$$

and pairs in each group are assigned a new bond with equilibrium distance equal to the mean distance of their region and a force constant equal to one-fifth of the regular value for the force field, see Table 1.

The relaxation is divided into five steps to gradually decrease the equilibrium bond length and increase the force constant of the new bonds to the DREIDING values (r_0 = 1.41 Å and k_0 = 350 kcal/mol, respectively, for C–N bonds in this system). Table 1 shows the bond parameters used in this multigroup multistep relaxation procedure. For each step, a 10 ps MD run is performed to relax the system. Such 50 ps procedure provides time for the system to adjust to its new topology. Dividing the new bonds into three groups based on their initial bond distance is important to avoid large interatomic forces as new bonds are formed. Fig. 3 shows the volume and instantaneous temperature fluctuations during the process of bond formation for a system containing 16 EPON and 8 DETDA molecules. We compare our approach with three groups of bonds at each of the five bond formation stages with a case where a single set of bonds parameters is used at each stage. Fig. 3 shows that using three groups of bonds together with a multistep procedure leads to significantly less fluctuations and has a less disruptive effect on atomic dynamics. Varshney et al. used a different bond type for each new bond; this approach is expected to lead to even smaller disruptions of the dynamics during bond creation as compared with our three-group method. The advantage of our approach lies in its computational simplicity and scalability. Since reactive pairs are grouped into three categories as opposed to creating a different bond type for every new bond, the number of bond types in our approach is independent of system size.

3.3. Chemical reaction models

As described above, the activation energy for reactions with primary amines is lower than that of secondary ones leading to

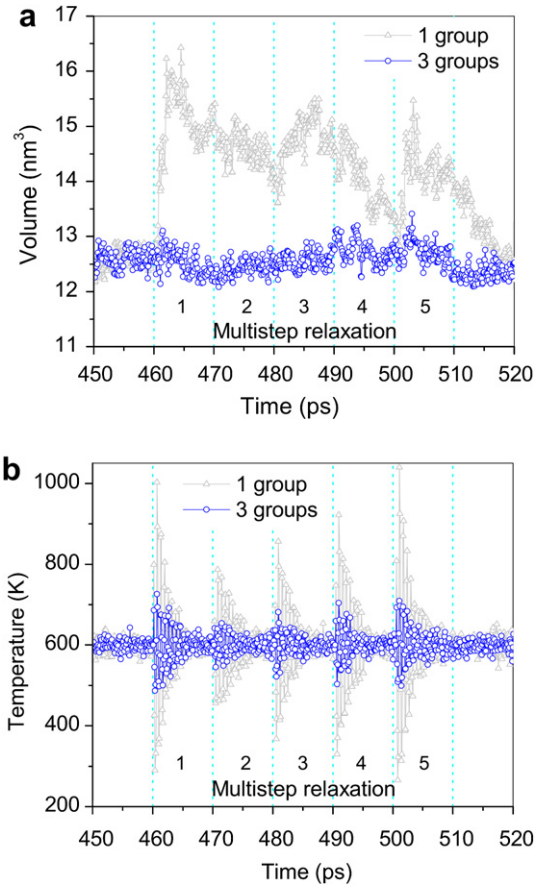

Fig. 3. Volume and temperature as a function of time during polymerization. The multigroup multistep relaxation effectively reduces the fluctuations during the creation of new bonds.

higher chemical reaction rates for the primary reaction. Actually, for low temperatures it is possible for the primary reactions to evolve to completion with little secondary reactions, which only occur at a significant rate when the reaction temperature is increased [17]. On the other hand, at high temperatures primary and secondary reactions are limited by mass diffusion and exhibit similar probabilities. An intermediate process occurs under normal production conditions, where the exothermicity of the curing process leads to an increase of the relative rate of secondary reactions.

In order to investigate how processing conditions affect the network and resulting properties we perform two types of conversion simulations: i) high temperature condition where primary and secondary reactions have equal probabilities (bonds are created between all reactive pairs within the cutoff distance); this processes is denoted *equal probability chemistry*. And ii) low to high temperature condition where for a pre-determined amount of time only reactions involving primary amines are enabled, followed by a second stage where all reactive pairs within the cutoff distance are reacted; this second approach is denoted *two-stage chemistry* model.

4. Partial atomic charges during conversion

Coulomb or electrostatic energy, calculated based on partial atomic charges, represents an important fraction of the total energy of many polymers. As described above, we expect charges to evolve during the polymerization and crosslinking procedure and they should be determined self consistently. In our simulations, the electronegativity equalization method (EEM), a semi-empirical approach parameterized using density functional theory (DFT) is adopted. Section 4.1 describes details of our implementation of EEM. Unfortunately charge equilibration models, including EEM, remain computationally intensive; this limits their use in large-scale MD simulations. However, one would expect atomic charges to be somewhat independent of the details of the environment and depend mostly on topology and chemistry; consequently significant charge evolution may only occur during chemical reactions. Our EEM-based polymerization simulations confirm this expectation and based on this observation we propose a new method that captures the physics of charge transfer in a computationally efficient; Section 4.2 describes this approach.

Table 2
EEM parameters.

Atom type	Electronegativity χ_i^* (eV)	Hardness η_i^* (eV)	Atomic size [26] $R_i = 14.4/2\eta_i^*$ (Å)
H	1.0	17.95	0.4011
C	5.25	9.0	0.8
N	8.8	9.39	0.7668
O	14.72	14.34	0.5021

4.1. EEM

The EEM is based on the electronegativity equalization principle that when two or more different atoms combine to form a molecule their electronegativities change to a common intermediate value [25]. In this study, the formalism of EEM developed by Mortier et al. [12] is adopted.

The EEM energy for an n-atom system is given by:

$$E(q) = \sum_{i=1}^{n}\left(E_i^* + \chi_i^* q_i + \eta_i^* q_i^2 + \frac{k}{2}\sum_{j\neq i}\frac{q_i q_j}{R_{ij}}\right) \quad (1)$$

where $E_i^*, \chi_i^* = (\frac{dE_i}{dq_i})_v$ and $\eta_i^* = (\frac{d^2E_i}{dq_i})_v$ are the coefficients of the Taylor expansion around the atomic value (asterisks indicate the values are from the Taylor expansion). χ_i^* and η_i^* represent the electronegativity and hardness of ith atom. The EEM electronegativity of an atom in the system is then given by the derivative of the energy with respect to the effective charge:

$$\chi_i = \left(\frac{dE}{dq_i}\right)_v = \chi_i^* + 2\eta_i^* q_i + k\sum_{j\neq i}\frac{q_j}{R_{ij}} \quad (2)$$

In Eqs. (1) and (2), q_i is the charge on atom i, χ_i is the equilibrium, environment-dependent electronic chemical potential of atom i, R_{ij} stands for the internuclear distance between atoms i and j. The constant k is a unit conversion factor, $k = 14.4$ gives energy in eV when distances are expressed in angstroms and charge in electrons. In equilibrium, all atoms should have the same chemical potential and for an n-atom system there are $n + 1$ unknowns (n atomic charges plus chemical potential) and n equations (Eq. (2)). The additional equation needed to solve the system of equations is $\sum_i q_i = 0$, which enforces charge neutrality. The most accurate descriptions modify the distance dependent on the electrostatic interaction term in Eqs. (1) and (2) to account for the finite-size of the charge distribution that leads to shielding for short distance and deviations from the $1/R_{ij}$ dependence [12,14].

There have been numerous studies on the calibration of parameters χ_i^* and η_i^* for various elements, usually using large training sets containing small organic molecules and finding a set of

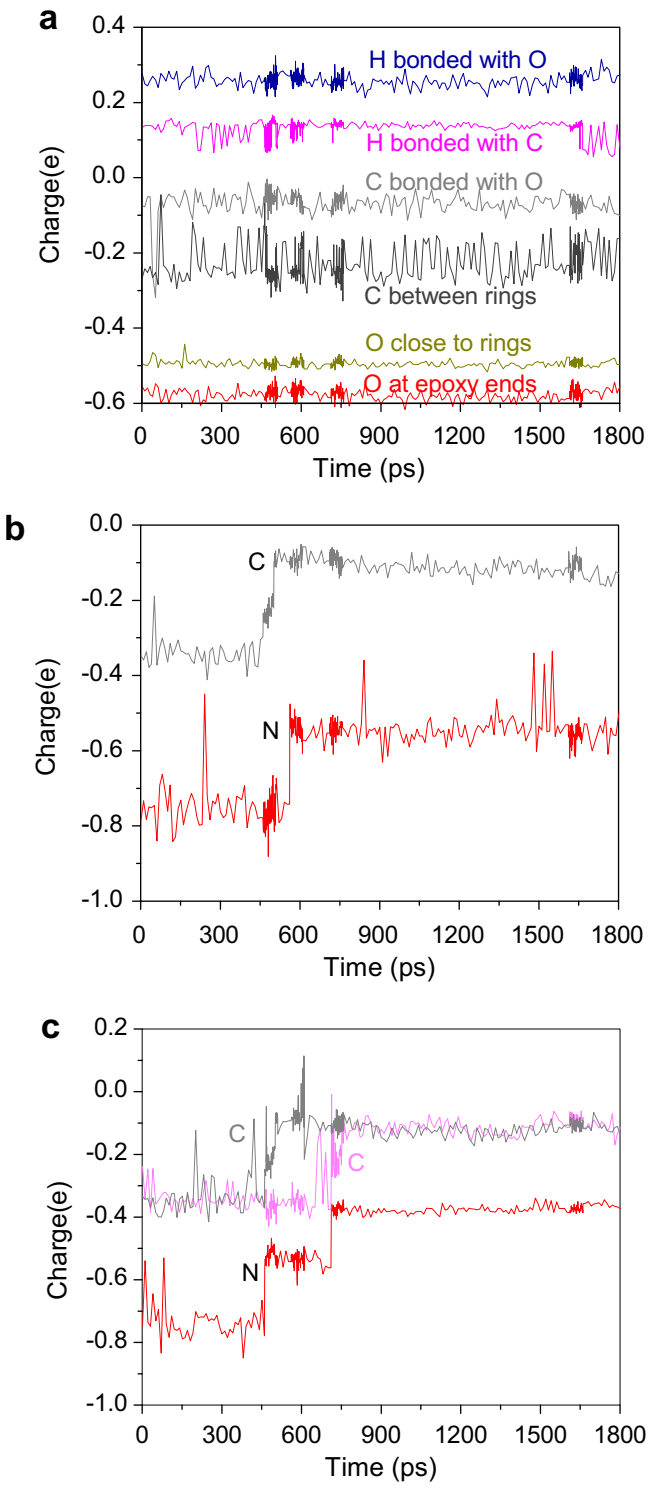

Fig. 4. Time evolution of partial charges on various atoms before and after reaction (a) Charges on atoms not involved in chemical reactions; (b) Charges on carbon and nitrogen atoms undergoing a primary reaction; (c) Charges on carbon and nitrogen atoms with primary and secondary reactions.

parameters that can give the best fit between the EEM and DFT charges. Although all parameterizations are applicable to our polymers, the parameters are often quite different from one set to another due to differences in training sets and optimization techniques used. Therefore, we tested various parameterizations on a set of small molecules; the parameters listed in Table 2 are employed in our simulations. These parameters are from Bultinck et al. [15], except that we use an expression for the internuclear distance R_{ij} that takes into account shielding corrections: $R_{ij}^{*} = \sqrt[3]{R_{ij}^3 + R_c^3}$. The shield radius is obtained from atomic values $R_c = \sqrt{R_i R_j}$ using an expression from Refs. [12,13], see Table 2.

During the polymerization and crosslinking procedure atomic charges are updated every 10 ps during the 50 ps equilibration stages and every 1 ps during the bond relaxation procedure.

4.2. EEM-based charge assignment (ECA)

Charge equilibration is a computationally intensive step in force field simulations and since it involves a matrix inversion it does not, in general, scale linearly with the number of atoms making it especially challenging for large-scale simulations. In this section we show that during polymerization and crosslinking EEM charges evolve in a relatively simple and predictable manner amenable to a simple parameterization based on atomic connectivities. The resulting method denoted EEM-based charge assignment (ECA) provides, once parameterized, a computationally efficient approach to describe charge evolution during polymerization.

During MD simulations EEM charges exhibit high-frequency oscillations around their equilibrium values due to thermal atomic motion and one would expect large charge variations when chemical reactions occur. An analysis of a polymerization/crosslinking run using EEM for a (16,8) system leads to the following general observations regarding charge distribution:

i) Charges on atoms not involved in chemical reaction undergo small fluctuations around their equilibrium values, as shown in Fig. 4(a).
ii) Charges on equivalent atoms fluctuate around the same average value.
iii) Charges on atoms involved in chemical reactions evolve only during the reaction in a predictable manner, as shown in Fig. 4(b) and (c).

This indicates that it should be possible to develop a scheme to assign partial charges and update those for atoms involved in chemical reactions with minimal computational overhead.

The first step in our approach is to determine the initial atomic charges for the unreacted epoxy resin and curing agent–liquid mixture. These are obtained from EEM charges during a pre-crosslinking run. The charge on each individual atom is time-averaged and as mentioned before atoms with equivalent chemical environments exhibit very similar charges and those are further averaged together. The initial charges for EPON-862 and DETDA based on our method are listed in the Appendix.

The second step involves updating atomic charges of the atoms involved in chemical reactions. Each reactive carbon in EPON-862 can react with a nitrogen atom in DETDA and each nitrogen atom in DETDA can form two new bonds with two EPON-862 carbon atoms; these reactions with nitrogen can happen simultaneously or not. Fig. 4(b) shows the temporal evolution of the charge of a reactive C/N pair and Fig. 4(c) shows a nitrogen atom that reacts with two carbon atoms at two different times. When a nitrogen atom bonds with one carbon atom, as shown in Fig. 5(a) and (b), its charge increases by 0.195 e, from −0.755 e to −0.56 e and the charge on the carbon atom changes by +0.2185 e from −0.3328 e to −0.1143 e. Note that the change in total charge is zero considering the charges on two hydrogen atoms that are removed during the chemical reaction, one from the nitrogen and another from the carbon. When a nitrogen atom forms two new bonds with carbon atoms, as shown in Fig. 5(c) and (d), its charge changes

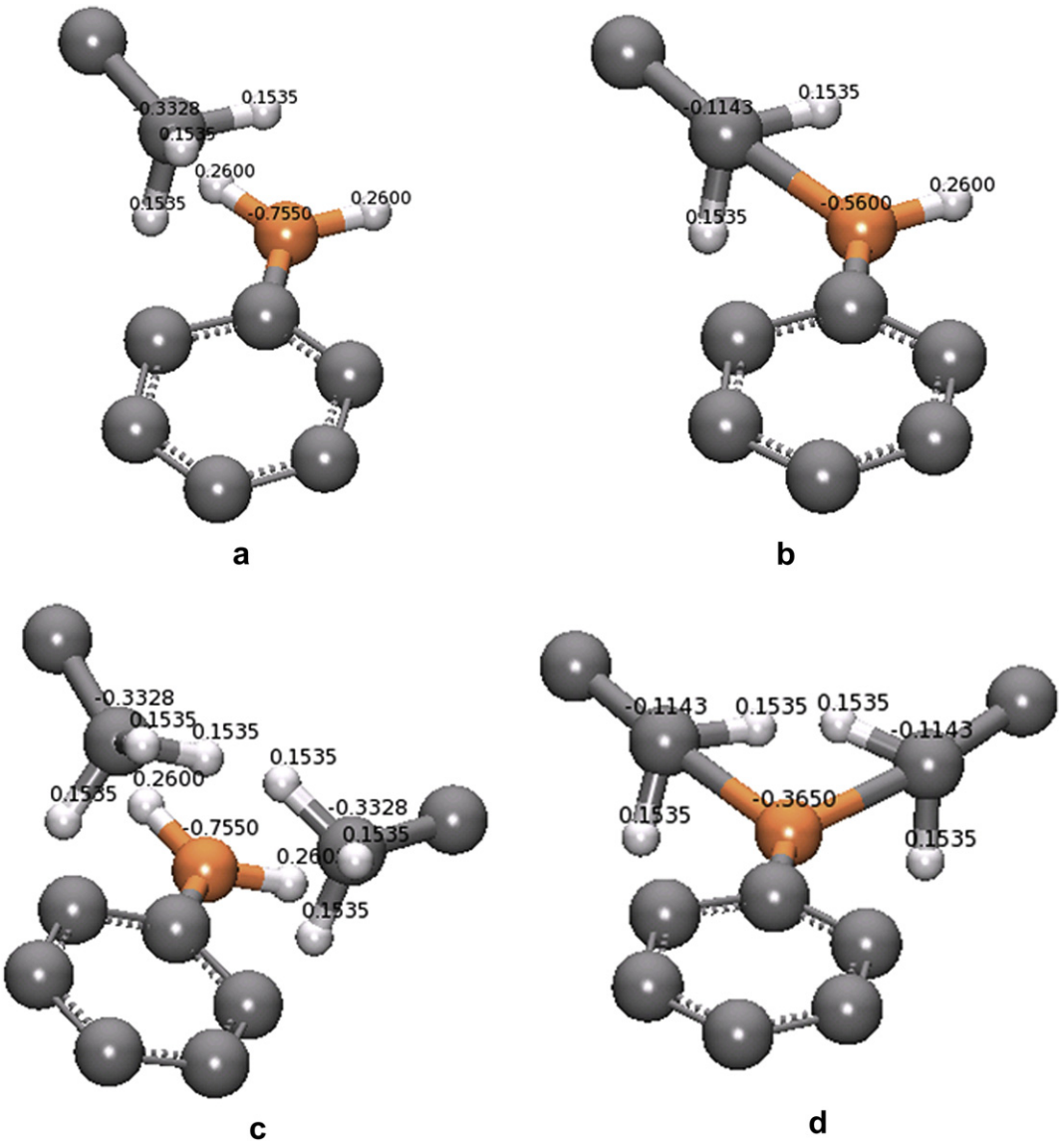

Fig. 5. Charges on atoms before and after reaction (a) and (b): DETDA reacting with one EPON; (c) and (d): DETDA reacting with two EPONs.

$+2 \times 0.195$ e from -0.755 e to -0.365 e and the charge on each of the two carbon atoms increases by $+0.2185$ e. The net charge change is also zero considering the charges on four removed hydrogen atoms. In summary, when a reaction occurs, the charge on a nitrogen atom increases 0.195 e whereas the charge on a carbon atom increases 0.2185 e. The change in atomic charge of other atoms during the reaction is negligible. Thus, ECA uses simple rules to describe the charge evolution during chemical reactions providing a computationally efficient alternative to EEM. As will be shown below ECA leads to polymerization/crosslinking results very similar to EEM both in terms of volume contraction and total energy evolution. A single polymerization simulation using EEM is required to parameterize ECA for a given set of monomer and curing agent and this can performed on a relatively small system; once parameterized ECA can be applied to much larger simulations cells.

It should be pointed out that ECA is similar to the approach reported in the paper of Varshney et al. [10] An important difference is that the ECA approach is parameterized based on self-consistent charge calculations during the actual process of polymerization in the condensed phase while charges in Ref. [10] are obtained from small model molecules in the gas phase (the actual method to obtain those charges was not described in detail, the authors point out that they use Insight II, a commercial molecular modeling software). Our detailed analysis of the charge evolution during polymerization in the condensed phase lends credence to the charge assignments in Ref. [10] and in our paper.

5. Polymerization and crosslinking results

5.1. Role of temperature and charge update on polymerization/crosslinking

We performed polymerization/crosslinking simulations using the equal probability chemistry approach for small model systems (16, 8) using both EEM and ECA charge updates and under various temperatures from 300 K to 600 K. The purpose of these simulations is to verify the feasibility of ECA method and characterize the role of simulation temperature on the network structure produced during polymerization and crosslinking.

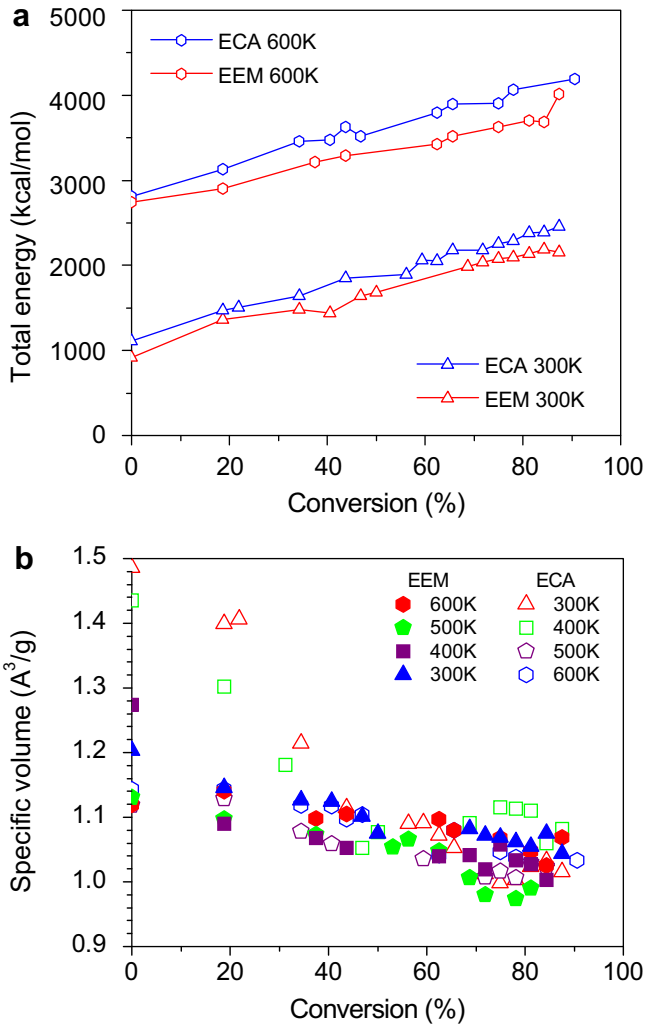

Fig. 6. Comparison of EEM and ECA for (16, 8) systems using the equal probability chemistry method and two different temperatures: (a) Total energy variations as a function of conversion; (b) Volume reduction as a function of conversion.

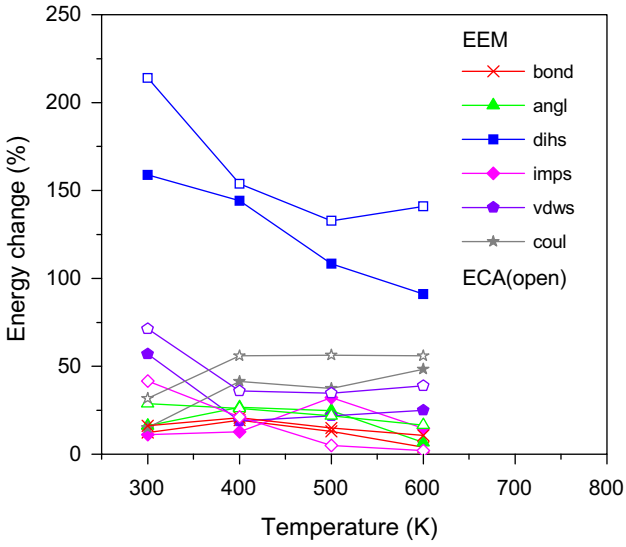

Fig. 7. Increase in energy components during polymerization as a function of temperature. ECA results show the change in energy from 0% to 87.5% conversion; EEM results show the change from 0% to 78.125%.

Fig. 6(a) shows the total energy as a function of conversion degree for two temperatures using both EEM and ECA. The conversion degree is defined as the number of new bonds formed out of maximum number of pairs of reactive sites. We find an increase in total energy with conversion degree in an approximately linear fashion. Both EEM and ECA exhibit the same trends and very similar increases in total energy during reaction. The total energy from ECA is slightly higher than that of EEM since EEM is able to adjust charges in response to the instantaneous configuration. An increase in total energy during polymerization and crosslinking may seem counter intuitive; the reason for this behavior is that the force field we use does not take into account the decrease in energy due to the formation of new bonds. Thus, since the number of covalent terms change with conversion, comparing total energies for different conversion degrees is meaningless. However, EEM and ECA energies for the same conversion degree can be compared and Fig. 6(a) shows that ECA leads to similar quantitative trends as the more computationally intensive EEM. Another important quantity to monitor during curing is the specific volume. At each step of the reaction we average the volume after the multistep relaxation and after the subsequent equilibration run; these average values are plotted along with the conversion degree in Fig. 6(b). As expected for small system sizes we see large fluctuations but volume shrinkage is clear as the crosslinking progresses. The shrinkage rate is in the range of 8–12% for 80–90% crosslinked polymers, which are all achieved with the cutoff distance predefined to $4r_0$ ($r_0 = 1.41$ Å). The EEM and ECA methods give essentially identical results on volume shrinkage.

In order to better understand how conversion proceeds during the simulation and optimize our approach we now focus on characterizing how the internal energy of the system evolves during conversion. As mentioned earlier, care should be taken when comparing energies of systems at different conversion degrees. DREIDING describes the total energy of the system as a sum of covalent terms (including bond stretch, angles, dihedral and improper torsions), van der Waals and electrostatics. Fig. 7 shows the percentage increase of the various energy terms during polymerization/crosslinking for various simulation temperatures. The bond, angle, dihedral and improper energies are each normalized by the actual number of terms for each conversion degree (i.e. bond energy per bond, angle energy per covalent angle, etc.). The van der Waals and electrostatics energy terms are normalized by the corresponding volume of unit cell. We find that all energy components increase during polymerization/crosslinking but the dihedral (torsions) energy plays a dominant role increasing over 100% of its original value. Furthermore, the increase becomes more important as the simulation temperature is decreased. These results show that dihedral energy dominates the total increase in internal network strain during the formation of the 3D crosslinked polymer indicating that these relatively floppy modes are forced away from their equilibrium value as the network forms and molecular groups loose mobility.

To confirm the trends observed in Fig. 7 regarding the role of temperature in the internal strain of the network and obtain a more direct measure of the degree of relaxation of structures built using different procedures, we compare the energy of a structure polymerized at $T = 300$ K (denoted low-T sample) and one polymerized at $T = 600$ K and then annealed to $T = 300$ K using a cooling rate of 10 K/200 ps (high-T sample). Both samples have the same degree of conversion (87.5%) and energies are averaged over 200 ps at $T = 300$ K. The total energy of the high-T sample is 2200 kcal/mol, 10% lower that that of the low-T sample, confirming that high temperature polymerization leads to a decrease in internal network

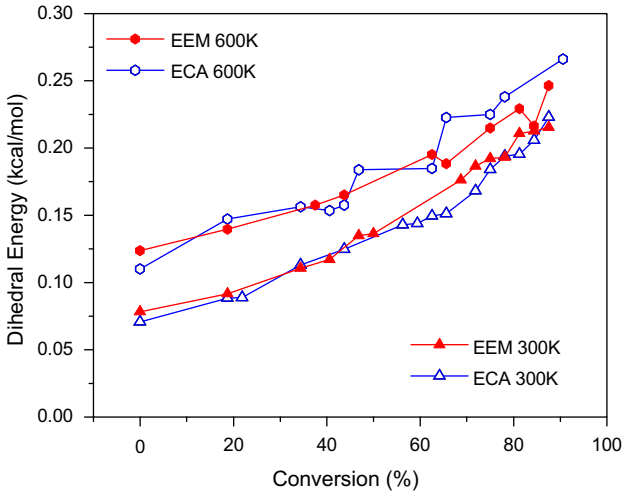

Fig. 8. Dihedral energy variations as a function of conversion.

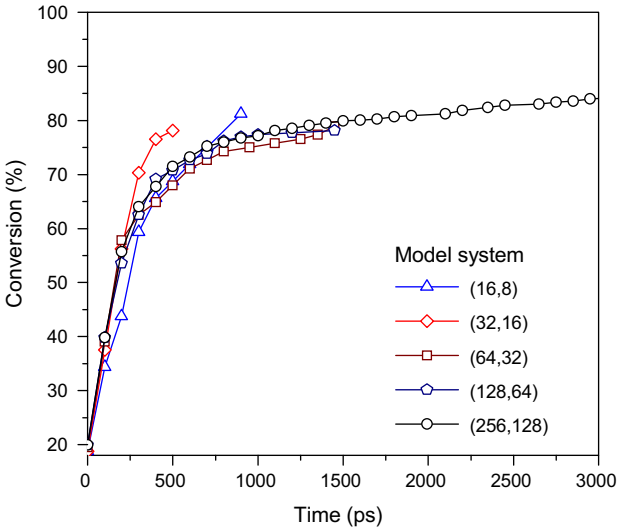

Fig. 10. Conversion degree vs. time for different sizes of model systems.

strain energy. The main terms contributing to this energy difference are bond angles (~20% difference) and dihedrals (~10% difference).

Fig. 8 shows the average dihedral energy per mode (covalent dihedral angle terms in the Hamiltonian) as a function of conversion degree for $T = 300$ K and 600 K both for EEM and ECA simulations. An interesting observation is that the rates of increase of internal network strain energy with conversion degree grow as the reaction progress. This implies that pulling molecules together as new bonds are formed becomes increasingly difficult as the network develops leading to increasing internal strain in the material.

5.2. Polymerization/crosslinking as a function of system size

We have shown that the ECA method is not only computationally efficient but also captures the role of charge evolution during reactions in the energetics and density of the polymers. Furthermore, we found that higher simulation temperatures are desirable since they lead to lower internal strain energies. Thus, now we focus on ECA simulations at 500 K and characterize the role of system size in the process of polymerization/crosslinking. Fig. 9 shows the specific volume as a function of reaction percentage for two different sizes; as expected, specific volume is not strongly dependent on size. The volume shrinkage for both sizes is about 10%, in good agreement with the simulation observation of Yarovsky and Evans [4] that a volume reduction of 5–12% occurs for various systems they simulated. Also, it is comparable to the 7% volume reduction reported by Varshney et al. [10] for larger systems. It should be pointed out that Varshney et al. did not observe volume shrinkage in small systems but our simulations show significant volume shrinkage even for small systems and the rate of volume shrinkage is largely independent of system size and temperature. Fig. 10 shows conversion degree as a function of time for systems of various sizes, from 1000 atoms for the (16, 8) system to 16 000 atoms for (256,128). As expected, conversion proceeds at a fast rate initially and this rate is essentially independent of systems size. The rate of conversion slows down significantly at 60–70% conversion as the mean separation between reactive sites increases and molecular mobility decreases due to the formation of the network. This range of conversion degrees where we observe conversion rate slowdown coincides with a steep increase in the molecular weight of the systems as described in Ref. [10].

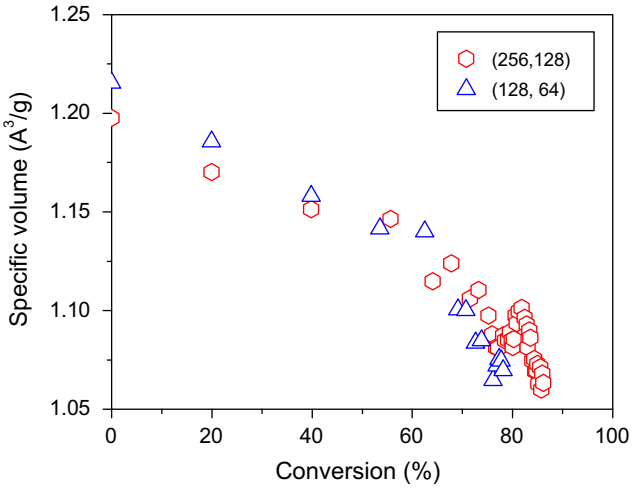

Fig. 9. Specific volume as a function of conversion for (128, 64) and (256, 128) systems.

5.3. Role of chemical kinetics

Fig. 11 shows the time evolution of the number of primary, secondary, and tertiary amines for the two chemistry models discussed in section 3.3. The equal probability chemistry model, Fig. 11 (a), shows secondary reactions starting at early times, as soon as secondary amines become available to react. On the other hand, Fig. 11(b) shows results from the two-stage model where secondary reactions are not allowed until primary reactions are almost fully completed (time 1.5 ns). Comparing these two extreme reaction models at an overall conversion percent of ~85%, we find for the equal probability model (corresponding to high curing temperature) 6.25% primary amines (unreacted) and 15.5% secondary amines (those that have undergone one reaction). The two-stage models lead to a lower number of primary amines (2.75%) with 23.5% of secondary amines. Interestingly, the number of tertiary (i.e. fully reacted) amines is similar in both cases: ~78% for the

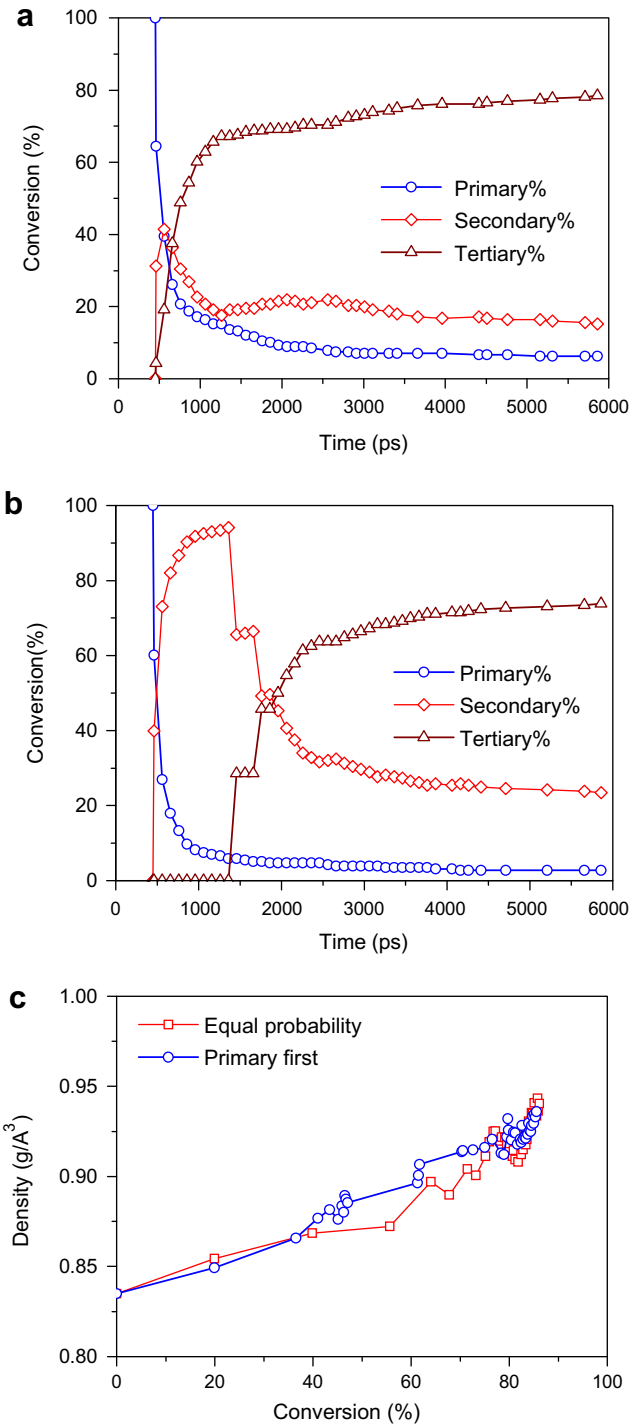

Fig. 11. Percentage of primary, secondary and tertiary amines as a function of time for the (a) equal probability and (b) two-stage chemistry models. c) Density as a function of conversion degree for the two chemistry models.

equal probability approach and ~74% for the two-stage model. Fig. 11(c) shows the density evolution during the process of conversion for the two chemical models. These simulations indicate that the density for the two-stage model is slightly higher than the equal probability approach for intermediate conversion degrees, in the range of 40–80%. For higher conversion degrees the two chemistry models lead to essentially identical densities. The likely reason for this observation is that when only reactions

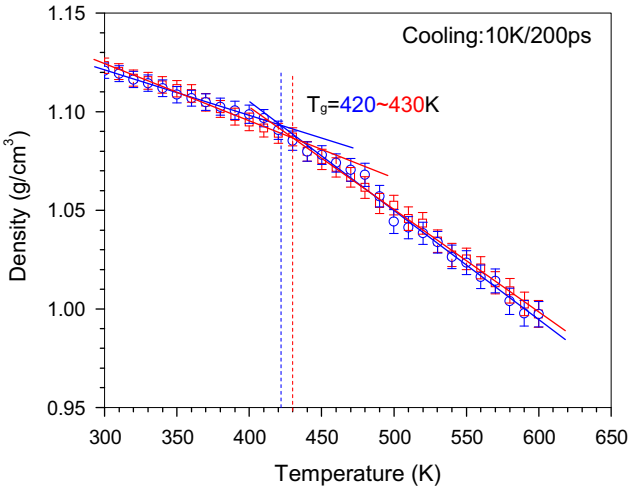

Fig. 12. Density as a function of temperature for X6 van der Waals interactions and for the two chemistry models: equal probability (red) and two-stages (blue) (for interpretation of the references to colour in this figure legend, the reader is referred to the web version of this article).

involving a primary amine are allowed, every reaction reduces the number of chain ends by two. This leads, in average, to a larger density increase than when a secondary amine reacts reducing the number of chain ends by one.

6. Thermo-mechanical properties of the resulting networks

In this section we characterize the thermo-mechanical properties of the resulting 3D network polymers. All these simulations are performed with the (256, 128) systems containing 15,198 atoms with a conversion degree of ~78%.

6.1. Glass transition temperature

After polymerization and crosslinking, the samples are cooled down to room temperature and the glass transition temperature and thermal expansion coefficient are obtained from these simulations. As described earlier these simulations are carried out using the Buckingham (X6) form for van der Waals interactions.

We cool down the system from 600 K to 300 K at a rate of 10 K/200 ps under atmospheric pressure. The density as a function of temperature is plotted in Fig. 12 for both chemistry models. The predicted density at $T = 300$ K (~1.12 g/cm^3) is in good agreement with the experimental value of (~1.17 g/cm^3) [27]. The change in slope of the density–temperature curves denotes the glass transition. To obtain the transition temperature and the error in this calculation, linear fits were performed to the MD density–temperature data below and above *Tg* in various temperature ranges. This procedure leads to a predicted T_g in the range 420–430 K for both chemistry models. These results show that the order in which chemical reactions occur has little effect on the room temperature density and the glass transition temperature for the high conversion degree tested here. For a slightly higher degree of conversion, 86%, the equal probability chemistry model leads to a slightly higher glass transition temperature of about 450 K.

The reported experimental T_g values of EPON-862/DETDA are 413 K [28], and 417–432 K [29]. The actual conversion degree of the

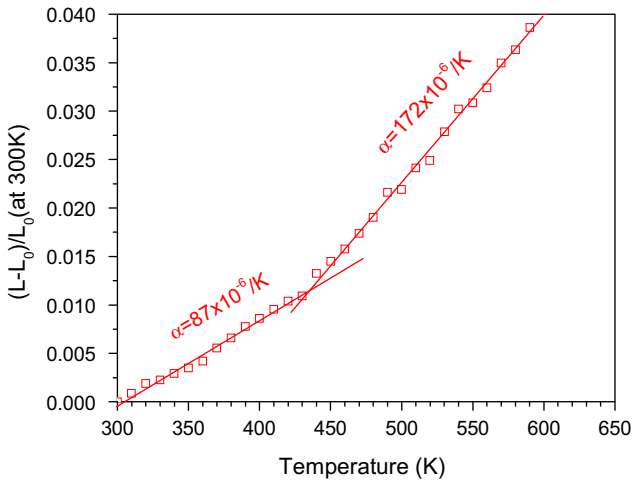

Fig. 13. Cell length normalized with $T = 300$ K value as a function of temperature for polymer with ~78% degree of conversion. Coefficients of thermal expansion before and after T_g are shown.

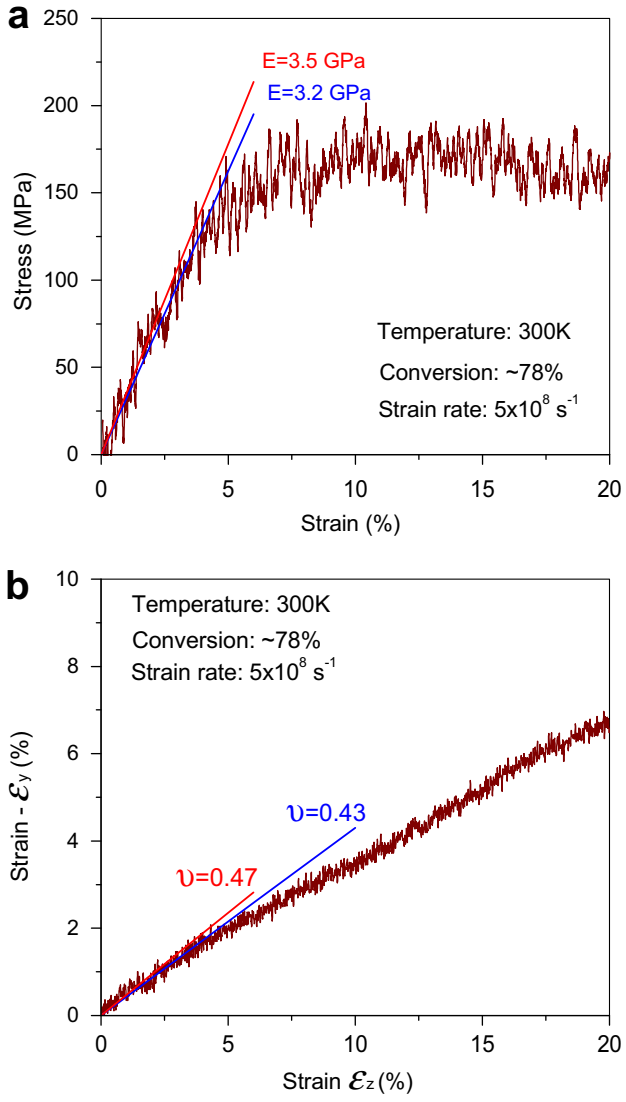

Fig. 14. Predicted stress–strain curve (a) and transverse strain vs. longitudinal strain (b) together with resulting Young's modulus and Poisson's ratio. A running average of the MD data with a 2 ps averaging period (strain of 0.095%) is shown to reduce the thermal fluctuations.

polymer tested in these experiments was not reported but typical values lie between approximately in the range 80–95% [17]. T_g is a kinetic quantity and depends on cooling/heating rate; an increase of 3 K is expected per order of magnitude increase in rate [30]. Thus, the T_g predicted from our MD (with a rate of 5×10^{10} K/s) should be about 30 K higher than the experimental value, i.e. the expected T_g for MD rates is 445–460 K. Our MD predictions, between 420 and 450 K, (for conversion degrees between 78 and 86%) using DREIDING are very close to this experimental range. In comparison, the T_g value given by Varshney et al. [10] using the CVFF force field is significantly lower (378 K).

6.2. Coefficient of thermal expansion

The coefficient of thermal expansion (CTE) can then be calculated from the simulation cell lengths during our isobaric cooling simulations described in Section 6.1, see Fig. 13. The simulation cell is maintained cubic throughout the simulation and an equal probability model is shown. The coefficient of linear thermal expansion is defined as:

$$\alpha = \frac{1}{L_0}\left(\frac{\partial L}{\partial T}\right)_P \tag{3}$$

where L_0 is the box size at 300 K and $(\partial L/\partial T)_P$ is the slope of linear part of the box size change vs. temperature. Our prediction for CTE using the Buckingham potential is 87×10^{-6} K^{-1} for temperatures below T_g and we find $\alpha = 172 \times 10^{-6}$ K^{-1} above T_g. Our calculations are in good agreement with experiments: 61×10^{-6} K^{-1} below and 195×10^{-6} K^{-1} above T_g [8]. Note that the accuracy of the MD predictions is higher above T_g where the polymer exhibits shorter relaxation times. Prior MD simulations on similar epoxy systems showed similar level of agreement with experiments, Ref. [10] predicts 40×10^{-6} K^{-1} at room temperature, and Ref. [8] 55×10^{-6} K^{-1} below T_g and 184×10^{-6} K^{-1} above T_g.

6.3. Elastic constants

We also calculated the elastic constants for the system described in the previous subsection (built using the equal probability chemistry model) via non-equilibrium MD simulations. We uniaxially strain the system while maintaining atmospheric pressure in the transverse directions and obtain the Young's modulus and Poisson ratio by fitting the MD data to linear functions up to strains within the linear response region of the system. Fig. 14(a) shows the MD engineering stress–strain curve for a strain rate of 5×10^8 s^{-1} up to 20% longitudinal strain and Fig. 14(b) shows transverse vs. longitudinal strains. As compared with experimental results for epoxy systems well below their glass transition temperatures the MD data in Fig. 14 exhibits a higher strength and lack of brittle failure. These are general features of all MD simulations of polymer systems cause by two key factors: i) the extremely large strain rates in MD (due to the limitations in total simulation time), and ii) the inability of the material to localize strain because of small sample sizes.

From the data shown in Fig. 14 we obtain a Young's modulus in the range 3.2–3.5 GPa and a Poisson ratio of 0.43–0.47. These ranges are obtained by fitting the MD data up to a maximum of various maximum strain values between 2% and 4%. The MD predictions are close to the experimental values reported for this system: Ref. [26] reports a Young's modulus of 2.76 GPa while Ref. [31] obtained an average Young's modulus of 2.65 GPa and a Poisson ratio of 0.35. As mentioned above, Wu and Xu [7] found extremely large elastic constants (~50 GPa) for DGEBA/IPD using

DREIDING with self-consistent charges, this result is inconsistent with ours results on EPON-862/DETDA and other polymers and might be erroneous.

7. Conclusions

In summary we proposed a method to mimic the process of polymerization and crosslinking in thermoset polymers based on MD simulations and characterized it via its application to the EPON-862/DETDA system. Our approach builds on previous efforts and provides justification to performing charge updates only during chemical reactions. We explored in detail, for the first time, how differences in chemical reactions related to processing conditions affect the resulting structures and thermal properties of the network. Our simulations show that whether primary reactions occur first followed by secondary ones or both reactions exhibit identical reaction rates from the onset does not affect the properties of the resulting network for conversion degrees higher than 80%.

Due to the limitation in timescales accessible to MD, the total simulation time for the polymerization/crosslinking processes is only a few nanoseconds, several orders of magnitude shorter than in experiments. The high rates of chemical reactions could lead to poor relaxation and larger internal strains in the network produced. Our results indicate that performing the simulations at high temperatures to increase molecular mobility mitigates this problem.

Using the general-purpose molecular force field DREIDING with Buckingham van der Waals interactions and EEM-based charges, our approach leads to predictions of density, glass transition temperature, thermal expansion coefficient, and elastic constants in good agreement with experiments. The predicted density is only slightly lower than the experimental value, this could be due to the high reaction rates used in the simulations; we are currently investigating how timescales affect the predicted properties. The glass transition temperature obtained from our MD simulations is between 420 and 430 K for a conversion degree of 78% and ~450 K for 86%. Once the effects of cooling rate are taken into account these results are within the experimental range. As noted in the original DREIDING paper, Buckingham van der Waals potentials lead to more accurate predictions than Lenard–Jones, which underestimates the density of the crosslinked polymer by about 10%.

Finally, the proposed approach is generally applicable to any thermoset system and we are currently applying it to other systems. Obtaining realistic atomistic structures of thermoset polymers is a key step towards the development of physics-based models that can be used to quantitatively predict and, eventually, optimize the properties of this important class of materials.

Acknowledgements

This work was supported by a grant with The Boeing Company and the US National Science Foundation (NSF) under contract CMMI- 0826356. Useful discussions with G. Medvedev, J. A. Caruthers, R. B. Pipes, S. Christensen and J. Goose and computational resources of nanoHUB.org are gratefully acknowledged.

Appendix

Initial charges on atoms of EPON-862 and DETDA.

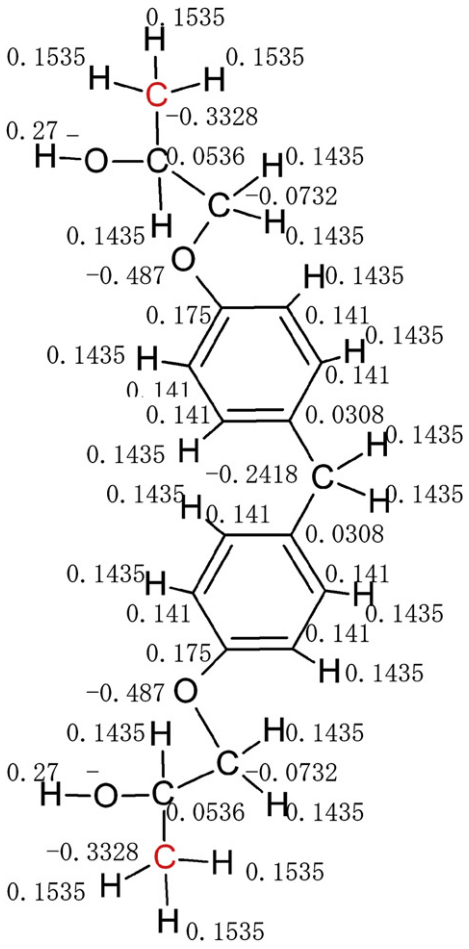

Fig. A1. Initial partial atomic charges on an EPON-862 monomer.

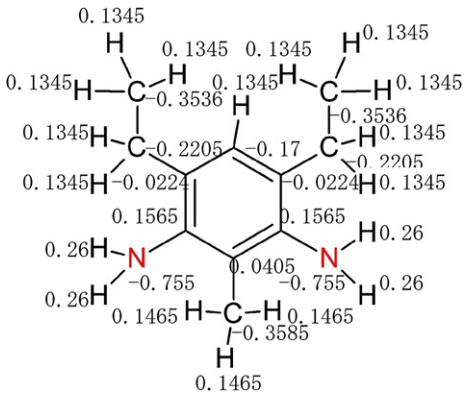

Fig. A2. Initial partial atomic charges on a DETDA monomer.

References

[1] Griffiths B. High Performance Composites. 2005;5:1–4.
[2] Pascault JP, Sautereau H, Verdu J, Williams RJJ. Thermosetting polymers. New York: CRC Press; 2002.
[3] Doherty DC, Holmes BN, Leung P, Ross RB. Comp Theor Polym Sci 1998;8:169–78.
[4] Yarovsky I, Evans E. Polymer 2002;43:963–9.
[5] Heine DR, Grest GS, Lorenz CD, Tsige M, Stevens MJ. Macromolecules 2004;37:3857–64.
[6] Gou J, Minaie B, Wang B, Liang ZY, Zhang C. Comp Mater Sci 2004;31 (3–4):225–36.
[7] Wu CF, Xu WJ. Polymer 2006;47:6004–9.
[8] Fan HB, Yuen MMF. Polymer 2007;48:2174–8.
[9] Lin PH, Khare R. Macromolecules 2009;42:4319–27.

[10] Varshney V, Patnaik SS, Roy AK, Farmer BL. Macromolecules 2008;41:6837–42.
[11] Komarov PV, Chiu YT, Chen SM, Khalatur PG, Reineker P. Macromolecules 2007;40:8104–13.
[12] Rappe AK, Goddard III WA. J Phys Chem A 1991;95:3358–63.
[13] Mortier WJ, Genechten KV, Gasteiger JJ. Am Chem Soc 1985;107:829–35.
[14] Njo SL, Fan JF, van de Graaf BJ. Mol Catal A Chem 1998;134:79–88.
[15] Bultinck P, Langenaeker W, Lahorte P, De Proft F, Geerlings P, Waroquier M, et al. Phys Chem A 2002;106:7887–94.
[16] Wang XR, Gillham JK. J Appl Poly Sci 1991;43:2267–77.
[17] Schiering DW, Katon JE. J Appl Poly Sci 1987;34:2367–75.
[18] Mayo SL, Olafson BD, Goddard III WA. J Phys Chem 1990;94:8897–909.
[19] Jang SS, Goddard WA. J Chem Phys C 2007;111:2759–69.
[20] Hockney RW, Eastwood JW. Computer simulation using particles. NY: Adam Hilger; 1989.
[21] MAPS (The Materials And Processes Simulations platform). Scienomics Inc.; 2008.
[22] LAMMPS (Large-scale Atomic/Molecular Massively Parallel Simulator), open source code, http://www.cs.sandia.gov/~sjplimp/lammps.html.
[23] Hoover WG. Phys Rev A 1985;31:1695.
[24] Hoover WG. Phys Rev A 1986;34:2499.
[25] Sanderson RT. Chemical bonds and bond energy. New York: Academic Press; 1976.
[26] Note: In using LAMMPS, the parameters for calculating atomic charge are denoted as and, where $\gamma_i = 1/R_i$.
[27] http://www.resins.com/Products/TechnicalDataSheet.aspx?id=3950.
[28] Sun L, Warren GL, O'Reilly JY, Everett WN, Lee SMD, Lagoudas D, et al. Carbon 2008;46:320–8.
[29] Tao K, Yang SY, Grunlan JC, Kim YS, Dang B, Deng Y, et al. J Appl Poly Sci 2006;102:5248–54.
[30] Ferry JD. Viscoelastic properties of polymers. New York: John Wiley & Sons Inc.; 1980.
[31] Tack JL. Thermodynamic and mechanical properties of EPON 862 with curing agent DETDA by molecular simulation. Master's thesis, Texas A&M University, 2006.